ISSN: 0067-2904

Computer Simulation for the Effects of Optical Aberrations on Solar Images Using Karhunen-Loeve polynomials

***Raaid Noffi Hassan[1], Huda Shaker Ali[2], Wafaa Hikmat Wadee[3]**
[1]Al-Karkh University of Science, Baghdad, Iraq,
[2]Department of Astronomy and Space, College of Science, University of Baghdad, Baghdad, Iraq,
[3]Departmen of Remote Sensing, College of Remote Sensing and Geophysics, Karkh University of Science, Baghdad, Iraq

Received: 8/5/2020 Accepted: 14/9/2020

Abstract

Numerical simulations were carried out to evaluate the effects of different aberrations modes on the performance of optical system, when observing and imaging the solar surface. Karhunen-Loeve aberrations modes were simulated as a wave front error in the aperture function of the optical system. To identify and apply the appropriate rectification that removes or reduces various types of aberration, their attribute must be firstly determined and quantitatively described. Wave aberration function is well suitable for this purpose because it fully characterizes the progressive effect of the optical system on the wave front passing through the aperture. The Karhunen-Loeve polynomials for circular aperture were used to describe wave front deviations and to predict the initial state of adaptive optics corrections. The results showed that increasing the aberration modes causes an increase in the blurring of the observed image. Also, we conclude that the optical phase error is increased significantly when aperture's radii are increased.

Keyword: Karhunen-Loeve, Zernike Polynomials, Wave Front Aberration, Solar Adaptive Optics, and PSF.

محاكاة حاسوبية لتأثيرات الزيوغ البصرية على الصور الشمسية باستخدام متعددة حدود Karhunen–Loeve

***رائد نوفي حسان[1], هدى شاكر علي[2], وفاء حكمت وديع[3]**
[1]جامعة الكرخ للعلوم, بغداد,العراق,
[2] قسم الفلك والفضاء,كلية العلوم, جامعة بغداد,بغداد,العراق
[3]قسم التحسس النائي,كلية التحسس النائي والجيوفيزياء , جامعة الكرخ للعلوم,بغداد,العراق

الخلاصة

تم تنفيذ محاكاة حاسوبية لتقييم تأثير انماط الغواشية المختلفة على المنظومة البصرية، خلال رصد وتصوير سطح الشمس. انماط الزيغ ل Karhunen–Loeve مثلت الخطأ في جبهة الموجة لدالة فتحة المنظومة البصرية. لتحديد وتطبيق التصحيح المرغوب للقضاء او خفض الانواع المختلفة للزيغ يجب اولاً اقتناص مميزاتها وصفاتها كميا. يناسب هذا الغرض بشكل جيد هو دالة غواشية الموجة لأنها تصف تماما

*raadnoffi742000@gmail.com

الاثر التراكمي للنظام البصري على الضوء الذي يمر من خلال كل موقع في الفتحة. تم استخدام متعددة حدود Karhunen–Loeve لفتحة دائرية لوصف الانحرافات في جبهة الموجة وللتنبؤ بالحالة الاولية لتصحيحات البصريات المطورة. اظهرت نتائج الدراسة عند زيادة انماط الغواشية سوف تزداد غواشية الصور المرصودة. استنتجنا ايضا، ان الخطأ البصري للطور يزداد بزيادة فتحة المنظار.

Introduction

Adaptive optics (AO) allow ground based telescopes to achieve their theoretical diffraction-limited resolution by compensating for the blurring effects of the Earth's atmosphere. Over the past two decades, the high angular resolution provided by AO coupled with the largest telescopes and modern science instruments became an important tool for studying and understanding our universe [1].

Using Karhunen-Loeve polynomials for generating atmospheric turbulence was introduced. This method takes into account the temporal and spatial effects of simulating atmospheric turbulence on the observed images [2]. In addition, the use of Karhunen-Loeve polynomials was introduced rather than using Zernike polynomials, as they are a statistically independent set of orthonormal polynomials [3]. The analysis is based on the decomposition of the distorted wavefront over the aperture in an orthonormal series with randomly independent coefficients [4].

Model Approach

In the case of a modal representation, the estimate represents a coefficient of an aperture function. The wave front is represented by a set of functions; each function is valid over the whole aperture. They have to be linearly independent; the phase can then be given by [5]:

$$\emptyset(x,y) = \sum_{k=1}^{K} a_k Z_k(x,y)$$

where a_k are the coefficients and Z_k are the functions. Karhunen-Loeve polynomials will be discussed to approximate the wavefront.

Karhunen-Loeve Polynomials

Karhunen-Loeve (KL) polynomials are each a sum of Zernike polynomials. However, they have statistically independent coefficients [6]. This is important due to the nature of atmospheric turbulence, as described by the Kolmogorov model following Kolmogorov statistics [7]. KL polynomials are given as [8]:

$$K_p(\rho,\theta) = \sum_{j=1}^{N} b_{p,j} Z_j \qquad \ldots\ldots\ldots (1)$$

where $b_{p,j}$ is the constructing matrix of KL polynomials (Table-1) and N is the number of Zernike orders in which the KL order j is represented.

Table 1- $b_{p,j}$ Matrix for Constructing KL Polynomials [9]

$b_{1,1} = 1$	$b_{7,18} = -0.277$
$b_{2,2} = 0.999$	$b_{7,31} = 0.043$
$b_{2,7} = -0.032$	$b_{7,48} = -0.003$
$b_{2,16} = 0.002$	$b_{8,10}$ =0.033
$b_{3,3} = 0.999$	$b_{8,19} = 0.955$
$b_{3,8} = -0.032$	$b_{8,32} = -0.297$
$b_{3,17} = 0.002$	$b_{8,49} = 0.050$
$b_{4,5} = 0.984$	$b_{9,2} = 0.033$
$b_{4,12} = -0.179$	$b_{9,7} = 0.955$
$b_{4,23} = 0.019$	$b_{9,16} = -0.297$
$b_{5,6} = 0.984$	$b_{9,29} = 0.050$
$b_{5,13} = -0.179$	$b_{9,46} = -0.004$
$b_{5,24} = 0.019$	$b_{10,3} = 0.033$
$b_{6,4} = 0.984$	$b_{10,8} = 0.955$

$b_{6,11} = -0.179$	$b_{10,17} = -0.297$
$b_{6,22} = 0.020$	$b_{10,30} = 0.050$
$b_{7,9} = 0.960$	$b_{10,47} = -0.004$

To make a realization of a wave front after being distorted by the Earth's atmosphere, Fried derived Zernike-Kolmogorov residual errors. Thus, a wave front can be represented as [10]:

$$wavefront(\rho,\theta) = \sum_{i=1}^{M} a_i \ K_i(\rho,\theta) \qquad \ldots\ldots\ldots(2)$$

The wavefront is now represented as a sum of KL polynomials with the Zernike-Kolmogorov residual error weights in the a_i's. The a_i's in Equation (2), which was calculated from the Zernike-Kolmogorov residual errors and Δj, were measured through many experimental procedures by Fried [3, 10], calculated by Noll, and given in Table-2 in terms of D/r_0. Thus, a realization of atmospheric turbulence can be simulated for different severities of turbulence and different apertures [4 and 9].
Compensation of the atmospheric seeing can be achieved using the technology of Adaptive Optics, a technique which is being pursued by every major ground-based observatory. The techniques of AO are those by which telescope optics are adjusted on a rapid time scale to compensate for distortions in the wavefront entering a telescope. It is also possible to apply postdetection corrections to images and achieve high angular resolution on bright sources with ground-based telescopes [11].

Table 2-Zernike-Kolmogorov residual errors [9, 4]

Zernike Mode	Zernike-Kolmogorov residual error
Tip	$\Delta_2 = 1.0299(D/r_0)^{5/3}$
Tilt	$\Delta_3 = 0.5820(D/r_0)^{5/3}$
Focus	$\Delta_4 = 0.1340(D/r_0)^{5/3}$
Astigmatism X	$\Delta_5 = 0.0111(D/r_0)^{5/3}$
Astigmatism Y	$\Delta_6 = 0.0880(D/r_0)^{5/3}$
Coma X	$\Delta_7 = 0.0648(D/r_0)^{5/3}$
Coma Y	$\Delta_8 = 0.0587(D/r_0)^{5/3}$
Trefoil X	$\Delta_9 = 0.0525(D/r_0)^{5/3}$
Trefoil Y	$\Delta_{10} = 0.0463(D/r_0)^{5/3}$
Spherical	$\Delta_{11} = 0.0401(D/r_0)^{5/3}$
Secondary Astigmatism X	$\Delta_{12} = 0.0377(D/r_0)^{5/3}$
Secondary Astigmatism Y	$\Delta_{13} = 0.0352(D/r_0)^{5/3}$
Higher orders (J>13)	$\Delta_J = 0.2944(D/r_0)^{5/3}$

KL functions are built on the basis of Zernike polynomial expansion. This approach allows to reduce KL equations combined into the system of linear algebraic equations which are expressed for matrix elements analytically in terms of hypergeomatric function [12].

Table 3- Karhunen-Loeve Polynomials up to 4th order [2]

order	Aberration mode
$K1$	Z_1
$K2$	$b_{2,2}Z_2 + b_{2,7}Z_7 + b_{2,16}Z_{16}$
$K3$	$b_{3,3}Z_3 + b_{3,8}Z_8 + b_{3,17}Z_{17}$
$K4$	$b_{4,5}Z_5 + b_{4,12}Z_{12} + b_{4,23}Z_{23}$
$K5$	$b_{5,6}Z_6 + b_{5,13}Z_{13} + b_{5,24}Z_{24}$
$K6$	$b_{6,4}Z_4 + b_{6,11}Z_{11} + b_{6,22}Z_{22}$
$K7$	$b_{7,9}Z_9 + b_{7,18}Z_{18} + b_{7,31}Z_{31} + b_{7,48}Z_{48}$
$K8$	$b_{8,10}Z_{10} + b_{8,19}Z_{19} + b_{8,32}Z_{32} + b_{8,49}Z_{49}$
$K9$	$b_{9,2}Z_2 + b_{9,7}Z_7 + b_{9,16}Z_{16} + b_{9,29}Z_{29} + b_{9,46}Z_{46}$
$K10$	$b_{10,3}Z_3 + b_{10,8}Z_8 + b_{10,17}Z_{17} + b_{10,30}Z_{30} + b_{10,47}Z_{47}$
$K11$	$b_{11,14}Z_{14} + b_{11,25}Z_{25} + b_{11,40}Z_{40} + b_{11,64}Z_{64}$

$K12$	$b_{12,15}Z_{15} + b_{12,26}Z_{26} + b_{12,41}Z_{41} + b_{12,65}Z_{65}$
$K13$	$b_{13,5}Z_5 + b_{13,12}Z_{12} + b_{13,23}Z_{23} + b_{13,38}Z_{38} + b_{13,62}Z_{62}$
$K14$	$b_{14,6}Z_6 + b_{14,13}Z_{13} + b_{14,24}Z_{24} + b_{14,39}Z_{39} + b_{14,63}Z_{63}$
$K15$	$b_{15,4}Z_4 + b_{15,11}Z_{11} + b_{15,22}Z_{22} + b_{15,37}Z_{37} + b_{15,56}Z_{56} + b_{15,79}Z_{79}$

Results and Discussion

The first 15 KL polynomials are written and shown graphically in Figure-1 using MATLAB R2012b.

The effects of turbulence from the point of view of the time-averaged Point Spread Function (PSF) of the atmosphere are considered. The PSF was simulated by taking the fast Fourier transform of the

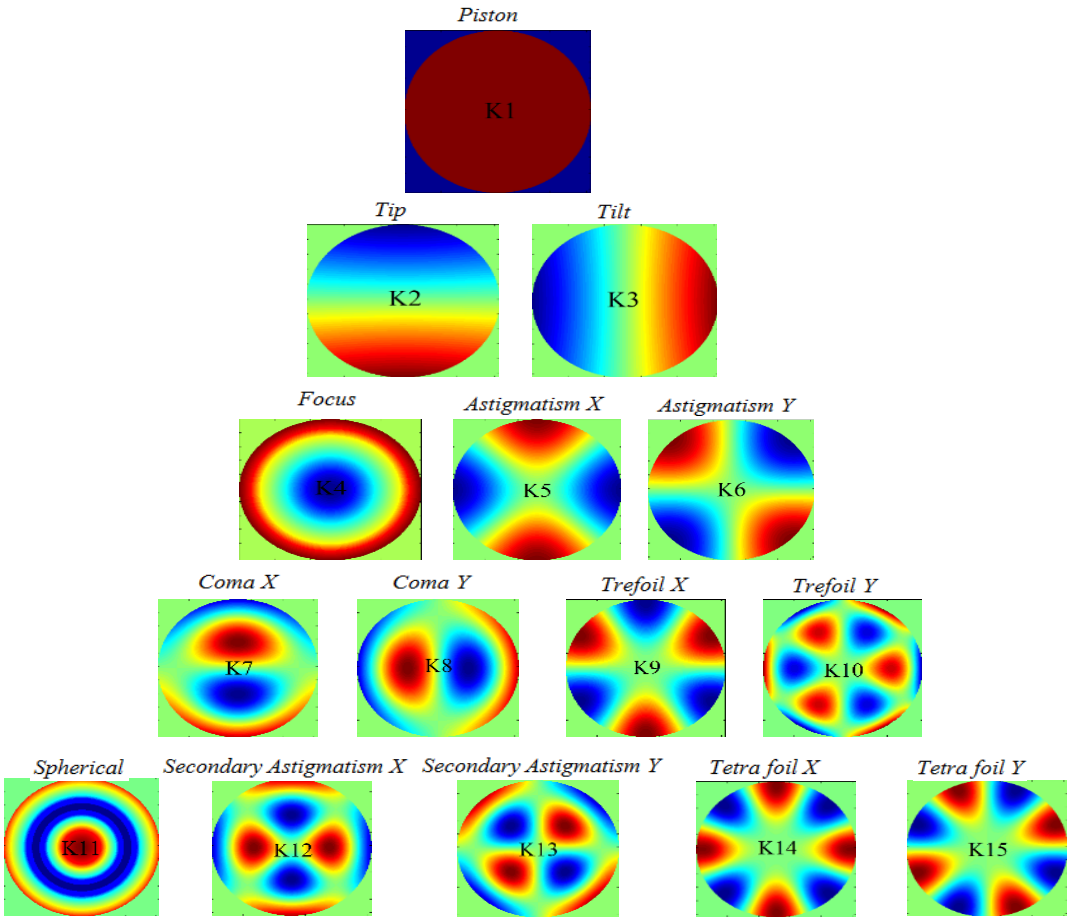

Figure 1- Graphical Representation of Karhunen-Loeve Polynomials up to 4th order.

pupil function that is associated with the optical phase error in terms of KL polynomials. Figures- (2-4) illustrate the estimated time average of the PSF for different types of aberrations KL modes (10 modes).

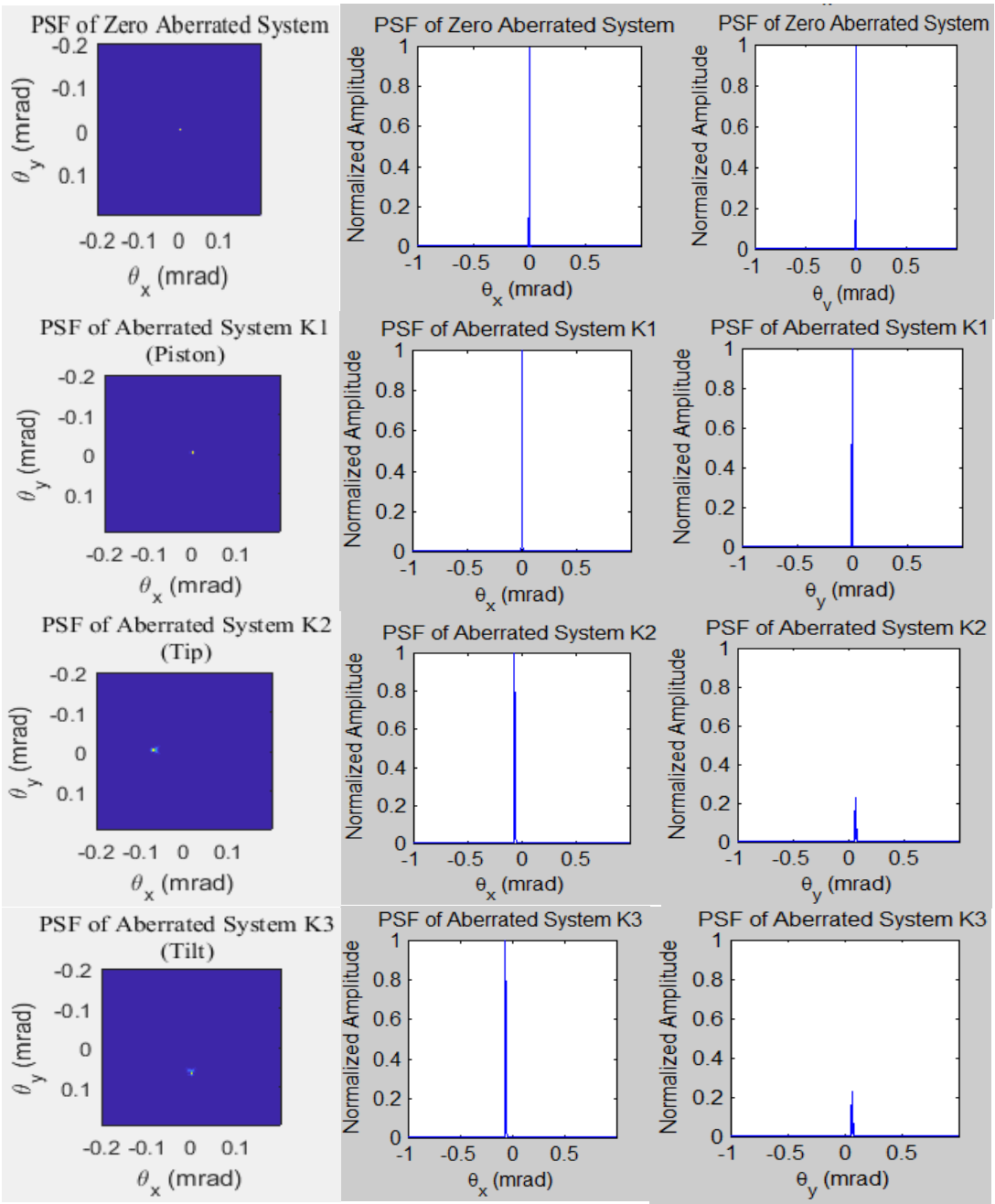

Figure 2-The PSF for aberrated circular aperture with KL modes K1- K3 (The first column is the image shape, the second column is the cross section in terms of visual angleθ_x and the third column is the cross section in terms of visual angleθ_y)

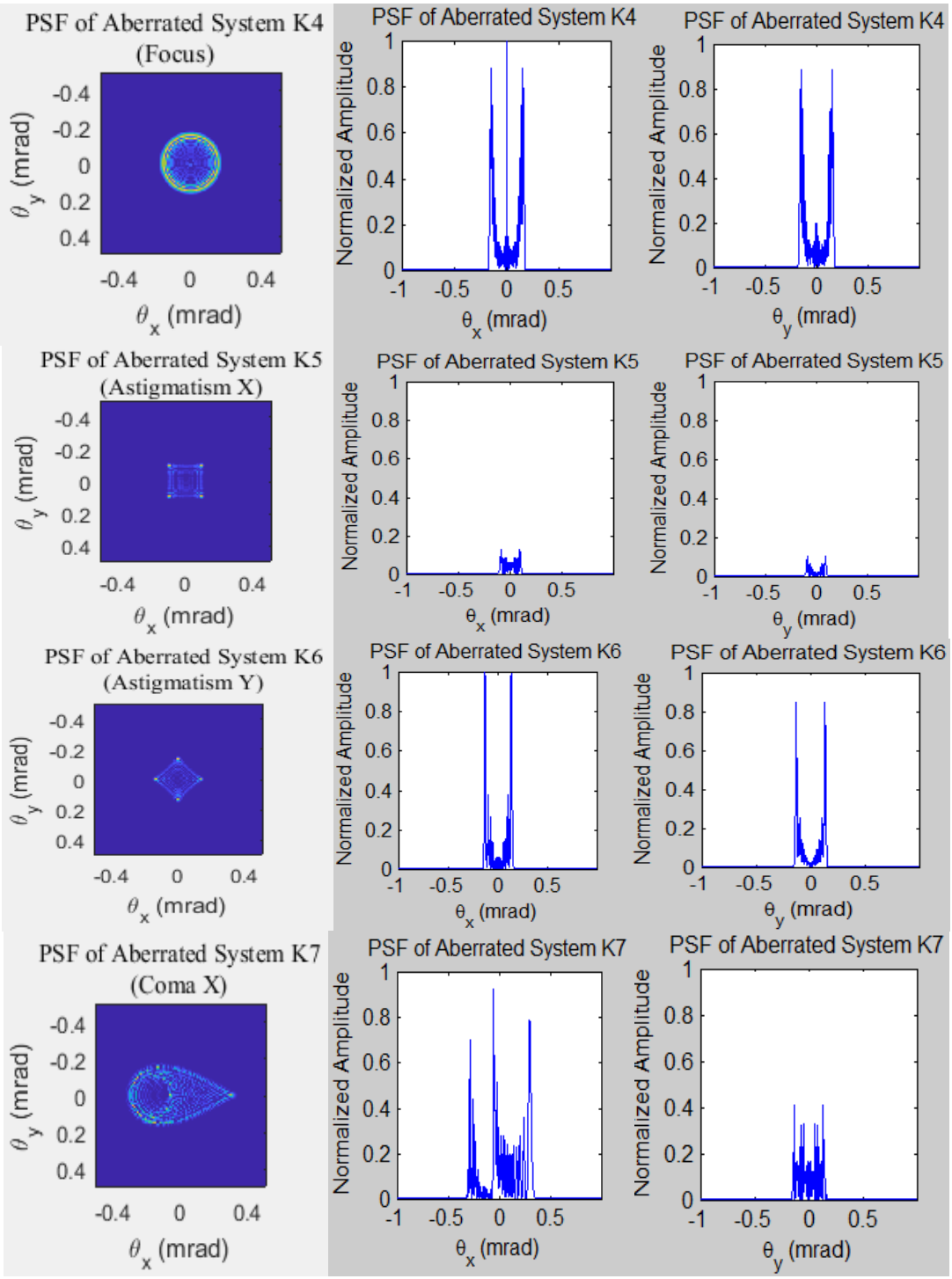

Figure 3-The PSF for aberrated circular aperture with KL modes K4 – K7 (The first column is the image shape, the second column is the cross section in terms of visual angleθ_x and the third column is the cross section in terms of visual angleθ_y)

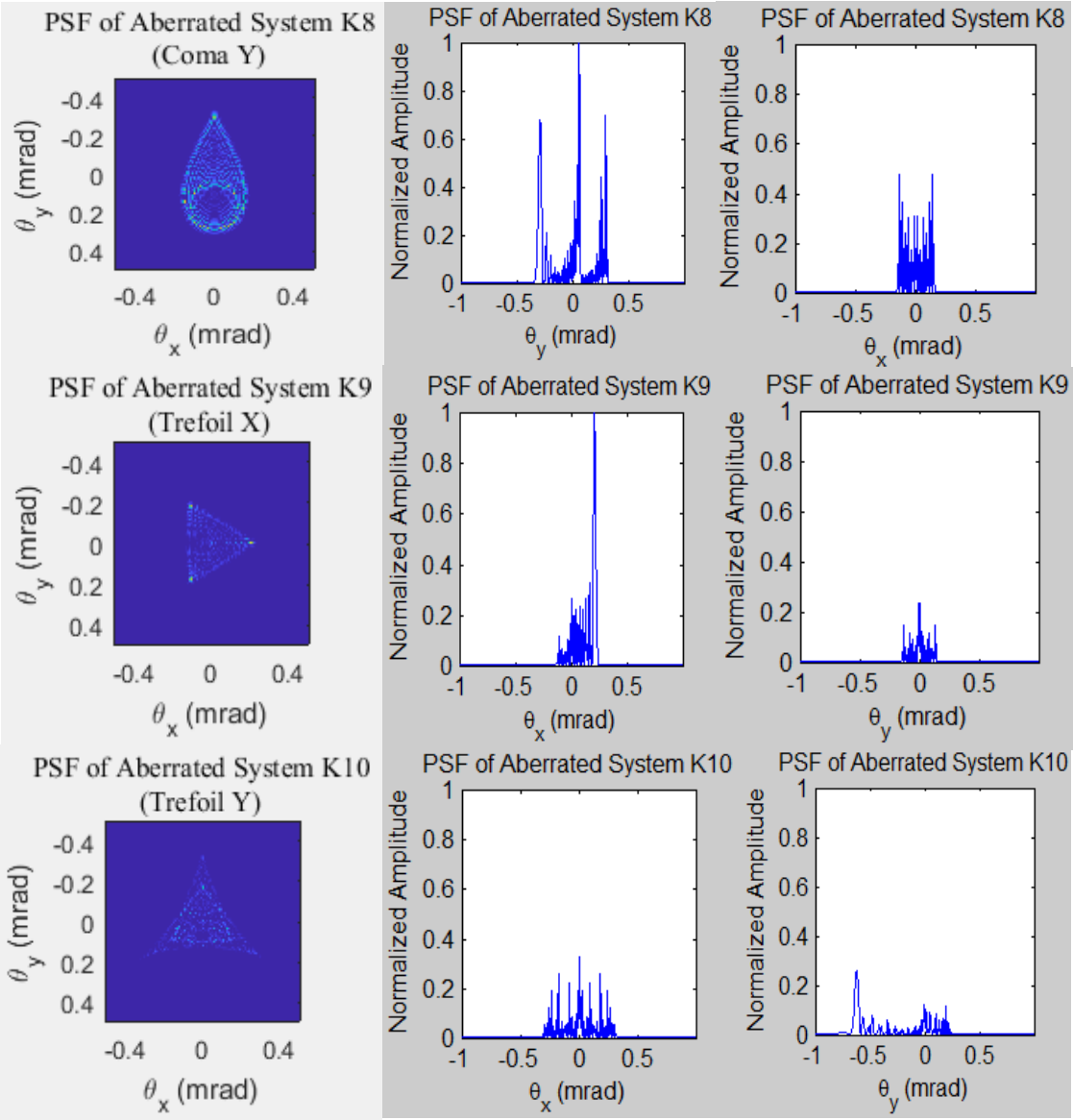

Figure 4- The PSF for aberrated circular aperture with KL modes K8 – K10 (The first column is the image shape, the second column is the cross section in terms of visual angleθ_x and the third column is the cross section in terms of visual angleθ_y)

As we know, the ideal shape of the PSF generally assumes perfect axial and rotational symmetry. Figures- (2-4) show the change rate of PSF shape as well as its wings and difference from the ideal state. However, it is quite close to the effect of each mode of the optical aberrations. In other words, PSF image shape is close to the shape of the aberration effect for each aberration mode (like defocus, astigmatism, coma, spherical aberration, and so on).

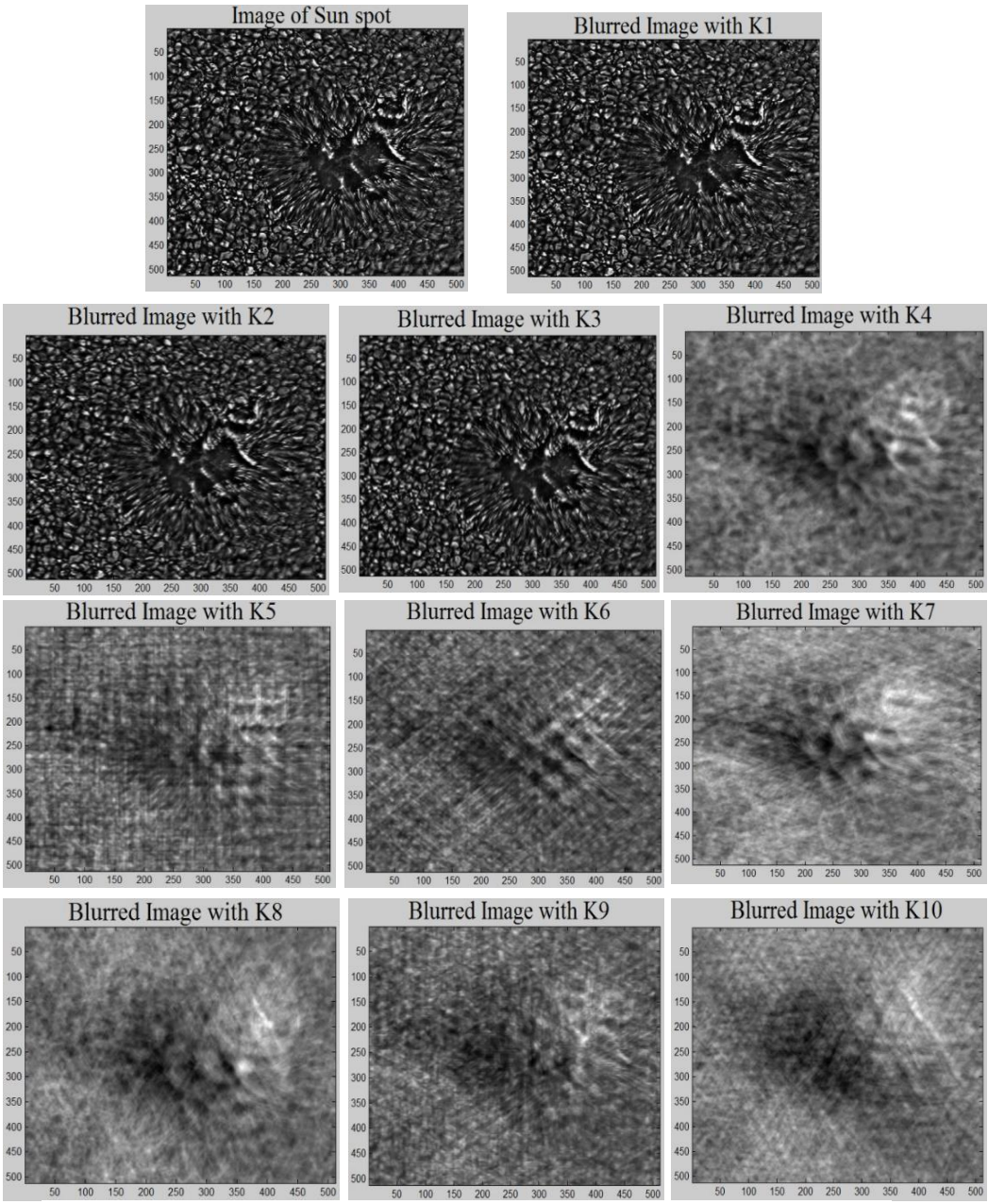

Figure 5-Convolution images with KL aberration modes.

Figure-5 shows the images of the solar surface in the presence of KL polynomials aberration modes (image convolution with polynomials). The convolved images show how the resolution of the observed image can be degraded under this condition.

Now, the comparative analysis of various quality metrics will be presented. In order to provide substantive results, evaluation with subjective measures requires careful selection of the test subject to correlate with human perception of image quality. Normalized Root Mean Square Error (NRMSE), Strehl Ratio (SR), Normalized Cross-Correlation (NCC) and Normalized Absolute Error (NAE) are the most commonly used criteria for image visual quality assessment. To investigate a relationship between the fidelity criteria and KL aberration modes (piston, tip, tilt, focus, astigmatism x, astigmatism y, coma x, coma y, trefoil x and trefoil y), Figures- (6, 7, 8, and 9) are used.

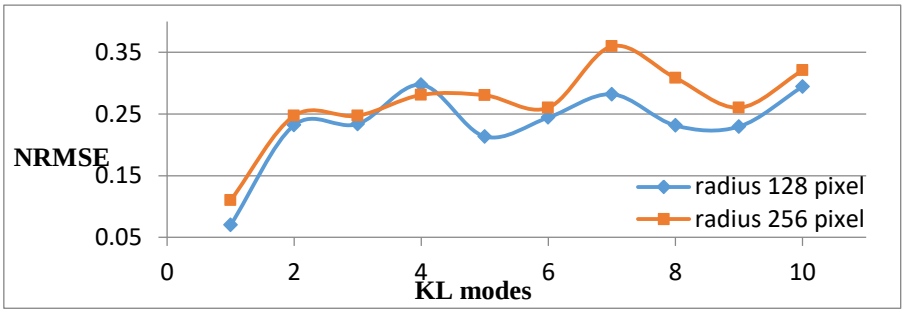

Figure 6- NRMSE vs. KL modes for two aperture radii

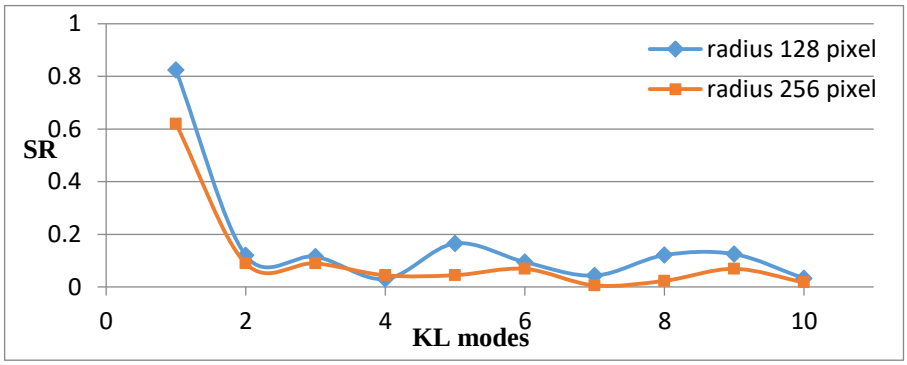

Figure 7-SR vs. KL modes for two aperture radii

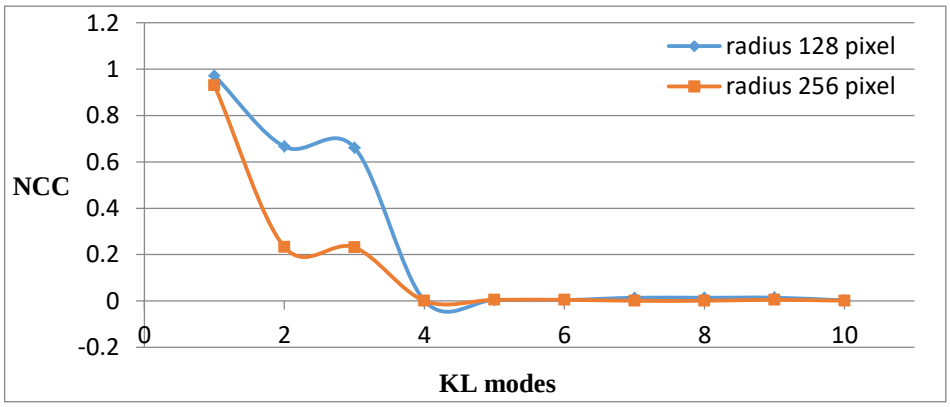

Figure 8-NCC vs. KL modes for two aperture radii

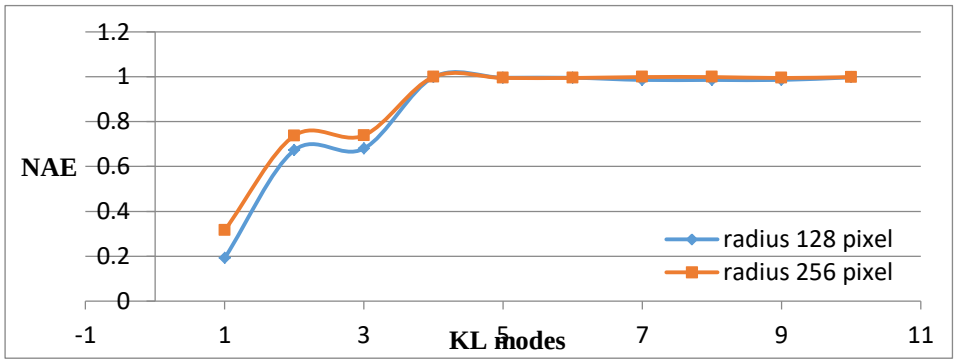

Figure 9-NAE vs. KL modes for two aperture's radii

In the above figures (6, 8, and 9) the fidelity criteria were proportional to the radius of the telescope's aperture, which means that with the increase of the telescope's aperture, the effect of the atmospheric turbulence will be increased. As we know, the SR metric parameter represents a measurement of the

optical quality. Figure-7 shows the decrease of SR with the increase of the aberration modes for both types of aperture radii, as expected. The difference between SR values for the piston mode KL1 for two aperture radii shows the high sensitivity for increasing the diameter of the telescope.
To study the relationship between a single aberration mode (focus K4) and aperture's radii for each objective fidelity criteria, Figures- (10, 11, 12, and 13) are employed.

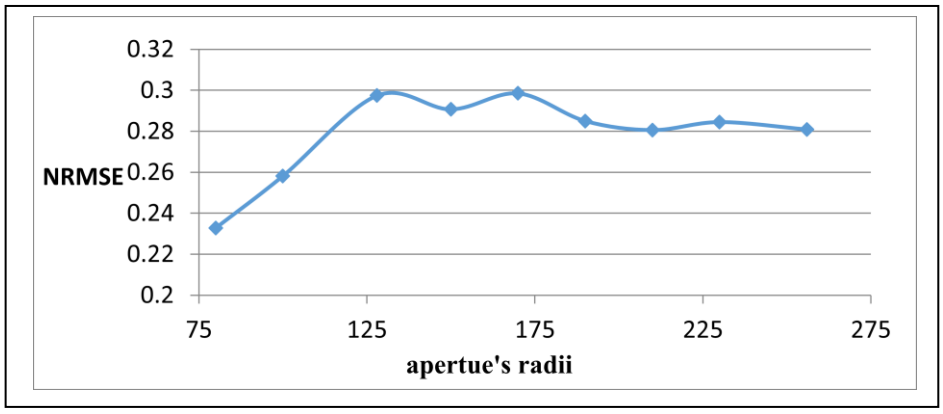

Figure 10- NRMSE for focus (K4) aberration mode vs. aperture radii

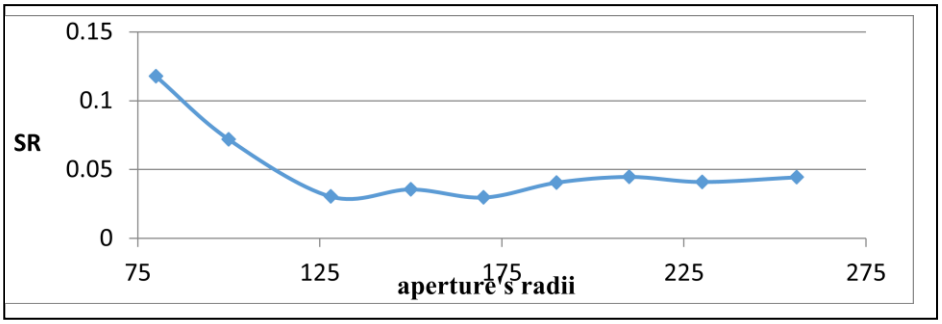

Figure 11-SR for focus (K4) aberration mode vs. aperture radii

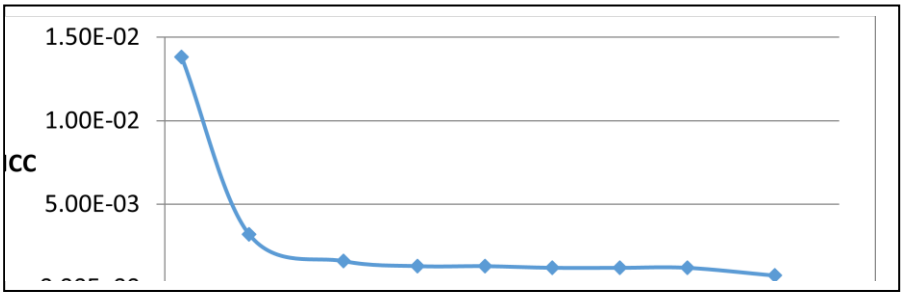

Figure 12-NCC for focus (K4) aberration mode vs. aperture radii

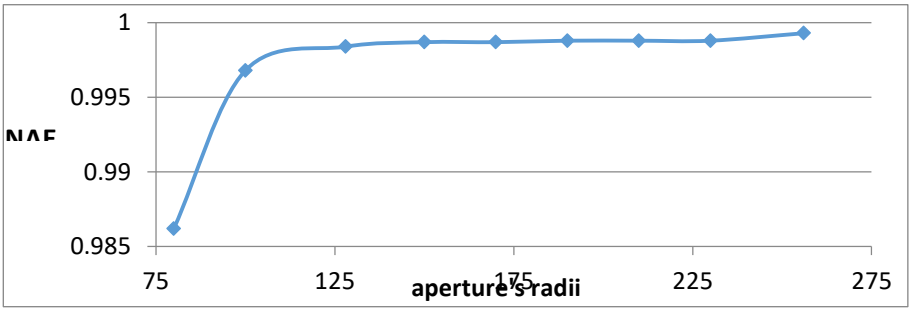

Figure 13-NAE for focus (K4) aberration mode vs. aperture radii

Conclusions

The simulations showed that the average PSF values for aberration circular aperture with KL modes from K1 to K10 (in Figures- 2, 3 and 4) and their effects on the original image (sun spot) were demonstrated in the convolved images in Figure-5. Clearly, increasing the aberration mode will cause an increase in the blurring of the observed image (sun spot). From Figures- (6, 7, 8, and 9) for both tow aperture's radii, it can be concluded that the optical phase error in terms of KL polynomials was increased with the increase of the aberration modes order.

Figures- (10, 11, 12, and 13) showed a relationship between the focus (K4) aberration modes as a function of aperture's radii. Evidently, it can be concluded that the optical phase error (focus) was increased significantly when aperture's radii were increased. When this increase is larger than 128 pixel radius, the behavior of the phase error is almost stable. Finally, the sum of all KL aberration modes can be used as an initial state of the adaptive optics process. The suggested future work to develop our simulation is to use multi-conjugate AO system for more reliable results.

References

1. Roddier. F. **1999**. "*Adaptive Optics in Astronomy*". Cambridge, Cambridge University Press.
2. Jallod, U. E. **2017**. "Simulations of Four Types of Optical Aberrations using Zernik Polynomials". *Iraqi Journal of Science*, **58**(1C): 583-591.
3. Wilcox ,C. C. **2009**. "Optical Phase Aberration Generation Using a Liquid Crystal Spatial Light Modulator". Ph. D. Thesis. College of Engineering, The University of New Mexico, United States.
4. Orlov, V. G. , Voitsekhovich ,V. V., and Cuevas , S., **1997**. "Karhunen-Loeve functions in simulations of atmospheric distortions". *Revista Mexicana de Astronomia y Astrofisica*, **33**: 187-195.
5. Visscher , G. **2014**. "Large scale wavefront reconstruction for the next generation of Extremely Large Scale Telescopes". M.Sc. thesis, Delft Center for Systems and Control, Delft University of Technology, Netherlands.
6. Toselli, I., Agrawal, B. N., Wilcox, C. C., and Restaino, S. **2011**. "Experimental generation of non-Kolmogorov Turbulence using a Liquid Crystal Spatial Light Modulator". Proceedings of the SPIE, 8161.
7. Stangalini, M., Moro, D. D., Berrilli, F. , and von der Lühe, O. **2010**. "Zernike basis optimization for solar Adaptive Optics using information theory*". Applied Optics*, **49**(11): 2090-2094.
8. Wang, J. Y. and Markey, J. K. **1978**. "Modal compensation of atmospheric turbulence phase distortion". *Journal of Optical Society of America*, **68**: 78-87.
9. Wilcox, C. C. , Restaino, S. R. , Martinez, T. , and Teare, S. W. **2013**. "*System and method of generating atmospheric turbulence for testing adaptive optical systems*". Patent No., 8452574 B2, US.
10. Noll, R. J. **1976**. "*Zernike polynomials and atmospheric turbulence*". *Journal of Optical Society of America*, **66**: 207-211.
11. Zhang, X. F., Wang, L. Q. **2014**. "Improvement in the performance of solar adaptive optics". *Research in Astronomy and Astrophysics*, **14**(4): 471-484.
12. Davies, R. and Kasper, M. **2012**. "Adaptive Optics for Astronomy". *Annual Review of Astronomy and Astrophysics*, **50**: 305-351.